

π -Donor Substituent Effects on Calculated Structures, Spin Properties, and Vibrations of Radical Anions of *p*-Chloranil, *p*-Fluoranil, and *p*-Benzoquinone

Scott E. Boesch and Ralph A. Wheeler*

Department of Chemistry and Biochemistry, and Center for Photonic and Electronic Materials and Devices, University of Oklahoma, Norman, Oklahoma 73019-0370

Received: June 18, 1997[⊗]

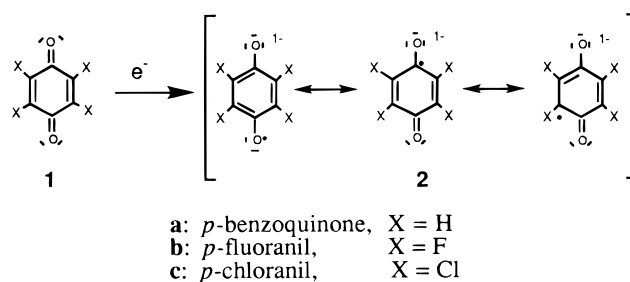
Vibrational and electronic properties of *p*-benzosemiquinone radical anions are important indicators of charge transfer in ion pairs, charge-transfer salts, and electron-transfer reactions. To provide missing data for radical anions of *p*-chloranil, *p*-fluoranil, and *p*-benzoquinone, and to test the capabilities of various computational methods, calculated structures, spin properties, and harmonic vibrational frequencies and mode assignments are reported based on molecular orbital, density functional, and hybrid Hartree–Fock/density functional computations. Qualitative structural changes upon reducing the neutral quinones to their semiquinone radical anions are predictable from the nodal structure of *p*-benzoquinone's LUMO. Furthermore, trends in calculated CO and C=C bond distance changes for the three molecules follow a pattern expected from the π -bonding abilities of the substituents. The most accurate calculated spin densities and isotropic hyperfine coupling constants show qualitative agreement with experimentally derived values for *p*-benzosemiquinone radical anion, whereas predicted spin densities and hyperfine coupling constants are reported for the other two species. Although calculated vibrational frequencies display small average absolute differences from experimentally measured frequencies (24 cm⁻¹ for *p*-chloranil's radical anion), for *p*-chloranil's radical anion calculations generally fail to reproduce several important details of the vibrational spectra.

Introduction

p-Benzoquinones find extensive use as electron acceptors in synthetic electron-transfer assemblies^{1,2} and charge-transfer salts.^{3–6} They are also ubiquitous in biological electron transfer.^{7–9} Plastoquinones and ubiquinones, for example, are substituted *p*-benzoquinones that function as electron acceptors for energy storage in the photosynthetic reaction center⁹ and energy utilization in mitochondria.^{10,11} Moreover, the radical anions of *p*-benzoquinones (see **1** for the neutral molecules)—*p*-benzosemiquinones (see **2**)—are increasingly used in fundamental studies of ion pairing in solution.¹² Identifying and characterizing the *p*-benzosemiquinone radical anions present in these various environments can be problematical and typically rely on measured vibrational frequencies^{13,14} and spin densities inferred from electron paramagnetic resonance (EPR) experiments.^{15,16} Although the *p*-benzoquinones are relatively well characterized,^{17–43} their corresponding radical anions, in general, are not. This contribution presents and compares calculated structures, electronic spin density distributions, and harmonic vibrational frequencies for the radical anions of *p*-benzoquinone (**2a**), *p*-fluoranil (**2b**), and *p*-chloranil (**2c**). Before presenting our results, however, we briefly summarize experimental data for the radical anions shown in **2** and the computational methods used.

Radical Anions of *p*-Chloranil, *p*-Fluoranil, and *p*-Benzoquinone

Although X-ray diffraction structures are available for crystals containing the radical anion of *p*-chloranil and alkali metal cations sequestered by crown ethers,⁴⁴ analogous structures for *p*-benzoquinone and *p*-fluoranil are to our knowledge unavailable. Moreover, the X-ray diffraction structures of *p*-chloranil's radical anion probably differ from the molecule's gas-phase



structure because close contacts between quinone oxygens and the alkali cations, evident in the crystal,⁴⁴ suggest strong interactions between the semiquinone anions and the alkali cations. Thus, the structure of *p*-chloranil's semiquinone anion⁴⁴ displays different bond lengths and angles at each end of the molecule, depending upon the distance between quinone oxygens and alkali metal cations. The quinone anion–alkali cation interaction is particularly evident in the C=O bond distances of 1.29 and 1.31 Å at each end of the molecule. The effect of the alkali cation is transmitted throughout the molecule, as even the C=C bonds are slightly affected by the oxygen atom's interaction with the metal cation, as the two carbon–carbon distances of 1.34 and 1.36 Å differ by 0.02 Å. Carbon–chlorine distances average 1.72 Å, but range from 1.66 to 1.80 Å. The high degree of disorder evident in the structure also makes the reported geometry imprecise, as standard deviations in bond distances of approximately 0.2 Å are quite large.

The sketch in **3** shows the atom number system subsequently used, spin densities inferred from EPR experiments in several aprotic solvents for the atoms of the *p*-benzosemiquinone radical anion,⁴⁵ and the oxygen atom's spin density for the radical anion of *p*-chloranil.⁴⁵ To our knowledge, analogous information for *p*-fluoranil's radical anion is unknown. For *p*-benzosemiquinone radical anion, the spin density is greatest on the oxygen atoms (0.161–0.166) and decreases for carbon atoms further from the oxygens. Thus the spin density on the oxygen-bearing C1/C1'

[⊗] Abstract published in *Advance ACS Abstracts*, October 15, 1997.

TABLE 1: Symmetries, Approximate Mode Descriptions, and Experimental Frequencies (cm⁻¹) for *p*-Benzoquinone, *p*-Fluoranil, and *p*-Chloranil Radical Anions^a

sym	approximate description	X = H	approximate description	X = F	approximate description	X = Cl
ag	C=C str	1620	C=C str	1677	C=C str	1594
b2u					C=C str	1545
b1u					C=O str	1525
ag	C=O str	1435	C=O str	1556	C=O str	1518
b1u					C-Cl str	1149
ag					C-Cl str	1028
b1u					C-C str	918
b2u					C-Cl str	722
b3u					C=O bend	695
ag	C-C-C bend	481			ring bend	517
b1u					C-Cl str	468
b2u					C=O bend	374
ag					C-C str	338
					C-Cl str	
b3u					C-Cl bend	220
b2u					C-Cl bend	212
b1u					C-Cl bend	200
ag	C-H bend	1161			C-Cl bend	

^a From refs 54–57.

atoms is 0.149–0.154, whereas the other carbons carry spin density of 0.092–0.093. These spin densities were inferred from measured proton hyperfine coupling constants (hfcc's), a rigorous measure of spin density at the hydrogen atom's nucleus. The measured proton hyperfine coupling constants for *p*-benzosemiquinone radical anion (–2.419 to –2.425) is expected to provide a more stringent test of computational methods than derived spin densities.^{46–53} For *p*-chloranil's radical anion, no hyperfine coupling constants are available for any magnetic nuclei, but the spin densities on oxygen (0.139–0.150) have been measured and are smaller than those on the oxygens of *p*-benzosemiquinone radical anion. Whether the remaining spin density on *p*-chloranil's radical anion resides on the carbon or the chlorine atoms is apparently uncertain.

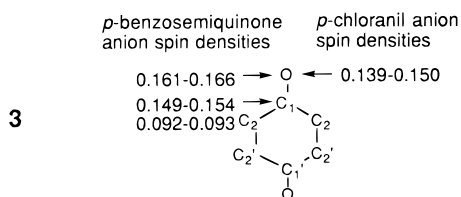


Table 1 compares experimentally determined vibrational frequencies, mode descriptions, and mode symmetries for the radical anions of *p*-benzoquinone,^{54–56} *p*-fluoranil,⁵⁵ and *p*-chloranil.⁵⁷ Only four vibrational frequencies, all with a_g symmetry, have been measured for *p*-benzosemiquinone radical anion.^{54–56} They include the in-phase CO stretch (1435 cm⁻¹), the in-phase C=C stretch (1620 cm⁻¹), a CH bend (1161 cm⁻¹), and a CCC bend (481 cm⁻¹). Comparing measured vibrational frequencies for *p*-benzosemiquinone radical anion with corresponding modes for the neutral *p*-benzoquinone molecule³⁸ provides insight into changes in chemical bonding upon one-electron reduction of *p*-benzoquinone, indicated in **1** and **2**. Thus, the in-phase C=O stretching frequency of 1663 cm⁻¹ for *p*-benzoquinone³⁸ is decreased by 228 cm⁻¹ in *p*-benzosemiquinone radical anion and indicates that the C=O bond is substantially weaker in the radical anion. Likewise, the C=C stretching frequency of 1657 cm⁻¹ is 37 cm⁻¹ higher for *p*-benzoquinone³⁸ than for *p*-benzosemiquinone radical anion and indicates a similar weakening of the C=C bond upon reduction of *p*-benzoquinone. The substantial increase in the a_g symmetry CCC bending mode's frequency in *p*-benzosemi-

quinone radical anion, compared to *p*-benzoquinone (447 cm⁻¹),³⁸ implies a more rigid carbon framework and indicates a more delocalized benzenoid structure for the radical anion compared to the neutral molecule. The virtually identical experimentally measured frequencies for the a_g symmetry CH bending mode of *p*-benzoquinone (1160 cm⁻¹)³⁸ and *p*-benzosemiquinone radical anion indicate that CH bonding is virtually identical in the two species.

Comparing experimentally measured vibrational frequencies for the tetrahalogenated *p*-benzoquinones and their radical anions, displayed in Table 1, allows similar inferences concerning differences in chemical bonding between the neutral and reduced species. For example, frequencies for the a_g symmetry CO stretching (1556 cm⁻¹) mode of *p*-fluoranil's radical anion have been experimentally measured, appear at lower frequencies than the CO stretching mode of *p*-fluoranil (1700 cm⁻¹),³⁵ and indicate weaker CO bonds for the radical anion. Although the a_g symmetry CC stretching frequency has been measured for the *p*-fluoranil radical anion (1677 cm⁻¹), this mode's frequency was not resolved for *p*-fluoranil.³⁵ For *p*-chloranil's radical anion, frequencies for both the a_g (1518 cm⁻¹) and b_{1u} (1525 cm⁻¹) symmetry CO stretching modes have been measured experimentally. Both the a_g (1594 cm⁻¹) and b_{2u} (1545 cm⁻¹) symmetry CC stretching modes were also detected. A variety of other vibrational modes—including C–Cl stretches, C–Cl bends, CO bends, an a_g symmetry ring bend (CCC bend, 517 cm⁻¹), a b_{1u} symmetry CC stretch (918 cm⁻¹), and a mixed CC and C–Cl stretch (338 cm⁻¹)—have been experimentally measured. In general, both CO stretching and both CC stretching frequencies are lower for the radical anion of *p*-chloranil than for the neutral molecule.³⁴ Thus, the a_g symmetry CO stretching mode of *p*-chloranil (1693 cm⁻¹)³⁴ appears 175 cm⁻¹ higher in frequency and the a_g symmetry CC stretching mode (1609 cm⁻¹)³⁴ appears 15 cm⁻¹ higher in frequency than the same modes of the radical anion. Furthermore, both the a_g symmetry CCC bend (496 cm⁻¹) and the b_{1u} symmetry CC stretch (908 cm⁻¹) for *p*-chloranil³⁴ were detected at lower frequencies (21 cm⁻¹ for the CCC bend and 10 cm⁻¹ for the b_{1u} symmetry CC stretch) than the analogous modes of the radical anion. Once again, this is entirely consistent with chemical bonding changes implied by the resonance structures shown in **1** and **2**.

Although qualitative differences in chemical bonding and vibrational frequencies between the neutral *p*-benzoquinones, **1**, and their radical anions, **2**, are available from their resonance structures, we seek a more detailed picture of bonding in the radical anions. Our calculations of structures, vibrational frequencies, and mode assignments for the radical anions of the *p*-benzoquinones shown in **2** allow comparison of the same properties not only of the neutral molecules but also between the three radical anions. Thus, this contribution fills gaps in our knowledge of the structures, vibrations, spin densities, and isotropic hyperfine coupling constants for the radical anions of *p*-benzoquinone, *p*-fluoranil, and *p*-chloranil; elucidates the effects of halogen substituents on chemical bonding and on physical properties of these radicals; and extends to halogenated *p*-benzosemiquinone radical anions our previous work to investigate the validity of various density functional (DF)^{58,59} and hybrid Hartree–Fock/density functional (HF/DF)^{58,60} methods for reproducing the structures and properties of quinones³ and their semiquinone anions^{46–49,61–63} and other cyclic, conjugated radicals.^{50–53,64,65}

Computational Methods

Several different local DF, gradient-corrected DF, and hybrid HF/DF methods were employed to compare their performance

to that of unrestricted Hartree–Fock (UHF), restricted open-shell Hartree–Fock (ROHF), and the second-order Møller–Plesset perturbation approximation for electron correlation (UMP2) for reproducing experimentally measured properties of cyclic, conjugated radical anions. Among the density functionals tested were the local spin density exchange functional of Slater (abbreviated S)⁶⁶ and the gradient-corrected exchange functional of Becke (B).⁶⁷ Correlation functionals used include the local density functionals of Vosko, Wilk, and Nusair (VWN)⁶⁸ and the gradient-corrected functional of Lee, Yang, and Parr (LYP).⁶⁹ In addition, the three-parameter hybrid HF/DF methods⁶⁰ denoted B3P86 and B3LYP (B3LYP results are reported as Supporting Information) were also tested. The three-parameter HF/DF methods employ a weighted sum of Hartree–Fock (E_X^{HF}), local DF (E_X^{Slater}), and gradient-corrected DF expressions for the exchange and correlation energies as follows for B3LYP:

$$E = aE_X^{\text{Slater}} + (1 - a)E_X^{\text{HF}} + b\Delta E_X^{\text{Becke}} + cE_C^{\text{LYP}} + (1 - c)E_C^{\text{VWN}}$$

where E_X^{Slater} is Slater's local spin density functional for exchange,⁶⁶ $\Delta E_X^{\text{Becke}}$ is Becke's gradient-corrected exchange functional,⁶⁷ E_C^{VWN} is the local density correlation functional of Vosko, Wilk, and Nuisair,⁶⁸ and E_C^{LYP} is the gradient-corrected correlation functional of Lee, Yang, and Parr.⁶⁹

The B3P86 method simply replaces Lee, Yang, and Parr's correlation functional with Perdew's 1986 correlation functional.⁶⁰ Coefficients giving the relative weights of various approximations for the exchange and correlation energies in the three-parameter method were optimized to reproduce thermochemical data for a variety of molecules, using one particular correlation functional, and may be found in the literature.⁶⁰ Throughout the paper, acronyms for the DF methods first indicate the form for the exchange functional followed by the form of the correlation approximation. For example, BLYP indicates Becke's exchange with Lee, Yang, and Parr's correlation functional. Except where indicated, all calculations were performed by using the 6-31G(d) split-valence plus polarization basis set.^{70,71} This basis was selected as a compromise between completeness and economy: it includes polarization functions on non-hydrogen atoms useful for modeling radicals, but it remains small enough for rapid calculations. However, one basis set tested here—Chipman's diffuse-plus-polarization basis denoted [632|41]^{72,73}—deserves special mention because it was developed specifically to model electron density near nuclei and therefore to yield accurate hyperfine properties of radicals in MO calculations. This contrasts with other, more commonly used Gaussian basis sets tested here, such as 6-311+G(d,p), designed to model electron density in the valence region and thus to describe chemical bonding.

Hartree–Fock^{70,74,75} or Kohn–Sham^{76,77} equations were solved by using the quantum chemistry computer programs GAUSSIAN92/DFT⁷⁸ or GAUSSIAN94.⁷⁹ Integrals required to solve the Kohn–Sham equations were evaluated by numerical quadrature on a grid of points by using the atomic partitioning scheme of Becke, without atomic size adjustments,⁸⁰ and using a standard grid of points.^{80,81} Berny's optimization algorithm⁸² was used to perform full geometry optimizations in C_1 symmetry using internal coordinates, followed by geometry optimizations in D_{2h} symmetry. Analytical first derivatives of the energy were computed to evaluate energy gradients in geometry optimizations, whereas analytical first and numerical second derivatives of the energy were used to calculate the Hessian matrix for vibrational frequency calculations in D_{2h} symmetry. Thus,

TABLE 2: Comparison of the Calculated Bond Distances and Bond Angles of *p*-Chloranil with the Calculated Bond Distances and Angles for the Radical Anions of *p*-Chloranil, *p*-Fluoranil, and *p*-Benzoquinone Determined by Using the B3P86 Hybrid Hartree–Fock/Density Functional Method with a 6-31G(d) Basis. Bond Lengths in Angstroms and Bond Angles in Degrees

	X = Cl	X = Cl	X = F	X = H
	Neut.	Anion	Anion	Anion
C=O	1.211	1.244	1.253	1.263
C=C	1.349	1.371	1.366	1.369
C–C	1.494	1.458	1.449	1.449
C–X	1.707	1.738	1.348	1.090
$\angle\text{O}=\text{C}-\text{C}$	121.4	123.0	123.5	122.7
$\angle\text{C}-\text{C}=\text{C}$	121.4	123.0	123.5	122.7
$\angle\text{C}-\text{C}-\text{C}$	117.2	114.0	113.0	114.6
$\angle\text{C}-\text{C}-\text{X}$	115.4	115.3	117.0	116.2

harmonic vibrational frequencies were evaluated at each level of theory for the molecules and radical anions discussed here. Although some workers scale calculated vibrational frequencies by a multiplicative factor to bring them into better agreement with experiment (and scaling factors appropriate for B3P86-derived frequencies (0.9556) have been determined⁸³), we prefer to report unscaled frequencies because in our experience some frequencies are lower than experiment and scaling does not necessarily improve overall agreement.

Whereas hyperfine coupling constants were calculated from Fermi contact spin densities, atomic spin densities for each radical anion were calculated by using Mulliken population analysis.⁸⁴ Because atomic charges calculated by using Mulliken population analysis are usually only qualitatively correct and depend on method and basis set size,⁸⁵ spin densities for *p*-benzosemiquinone radical anion were also calculated by using Bader population analysis.⁸⁶ Unlike Mulliken population analysis, Bader's method partitions space to determine the charge or spin on an atom, so we hoped that Bader's method would yield spin densities closer to experimentally derived spin densities. Bader population analysis was accomplished by using the program GAUSSIAN94.⁷⁹

Although some attempts were made to investigate the effects of including more polarization functions and diffuse functions in the basis set, more sophisticated methods with larger basis sets may be desirable to improve agreement with experiment.

Radical Anions of *p*-Chloranil, *p*-Fluoranil, and *p*-Benzoquinone-Structures

Table 2 presents a comparison of calculated structures of the radical anions of *p*-chloranil, *p*-fluoranil, and *p*-benzoquinone with each other and with the calculated structure of the neutral *p*-chloranil molecule. Since previous results indicated that the DF and HF/DF methods yield excellent bond distances for the neutral quinones,^{46–49,61,62} we will describe the calculated structure for *p*-chloranil very briefly. Although a variety of DF and HF/DF methods were employed, we will emphasize results obtained by using the hybrid B3P86 method because it appears to give the best overall agreement with experiment.

First, the calculated bond distances for *p*-chloranil are in excellent agreement with distances determined by electron diffraction.¹⁸ The calculated CO distance is 0.005 Å too short and the calculated C2C2' distance is also slightly too short, by 0.004 Å (to avoid confusion with chlorine, atom number one is omitted from the carbon bonded to oxygen and C2C2' defines the shorter pair of carbon–carbon bonds, as indicated in **3**). In contrast, the calculated CC2 distance, represented as a single bond in the Lewis structure of **1**, is only 0.002 Å longer than the experimentally determined distance. The calculated C2–Cl distance shows the poorest agreement with experiment, but

TABLE 3: Calculated Bond Distance and Bond Angle Changes upon Reducing *p*-Benzoquinone and *p*-Fluoranil to Their Radical Anions, Determined by Using the B3P86 Hybrid Hartree–Fock/Density Functional Method with a 6-31G(d) Basis Set. Bond Distance Changes in Angstroms and Bond Angle Changes in Degrees

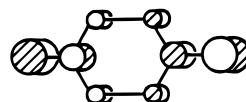
	X = H	X = F
C=O	0.041	0.040
C=C	0.028	0.023
C–C	–0.032	–0.032
C–X	0.004	0.028
∠O=C–C	1.4	1.8
∠C–C=C	1.4	1.8
∠C–C–C	–2.8	–4.2
∠C–C–X	0.3	1.6

differs from the electron diffraction result only by 0.006 Å. Bond angles calculated by using the B3P86 method also agree well with experiment and differ by an average of 0.2° and a maximum of 0.4° (for the C–C2–Cl angle).

Adding an electron to *p*-chloranil to form its radical anion changes bond distances in ways consistent with the resonance structures shown in **1** and **2**. The calculated CO distance expands significantly (0.033 Å) from 1.211 to 1.244 Å and the C2C2' bonds of *p*-chloranil lengthen from 1.349 to 1.371 Å in the radical anion (by 0.022 Å). The calculated C2C2' distance for *p*-chloranil radical anion thus falls almost midway between the experimentally determined C=C double-bond distance of *p*-benzoquinone (1.344 Å)¹⁷ and the experimental CC distance in benzene (1.396 Å).⁸⁷ The CC2 bond of *p*-chloranil contracts from 1.492 Å (in *p*-chloranil) to 1.458 Å (in the radical anion) and therefore resembles *p*-benzoquinone's CC2 single-bond distance (1.481 Å) more than the CC distances observed for benzene. Thus, the CO distance expands, whereas the carbon framework changes toward a benzenoid (or phenolic) structure upon reducing *p*-chloranil to its radical anion. Furthermore, the calculated C2–Cl distance of *p*-chloranil radical anion is 0.031 Å longer (1.738 Å) than the corresponding calculated distance in *p*-chloranil (1.707 Å).

Bond distance changes calculated upon reducing *p*-fluoranil and *p*-benzoquinone to their respective anions (see Table 3) are similar to those described for *p*-chloranil, but some trends for the three molecules are also discernible. First, the calculated CO and C2C2' bond distances for *p*-fluoranil lengthen by 0.040 Å (from 1.213 Å in *p*-fluoranil to 1.253 Å in its radical anion) and 0.023 Å (from 1.343 Å in *p*-fluoranil to 1.366 Å in the radical anion), respectively. The calculated CC2 distance in *p*-fluoranil's radical anion (1.448 Å) is also contracted, by 0.036 Å, compared to the same distance in *p*-fluoranil (1.484 Å). As with *p*-chloranil, the C–X (X = F) bond in *p*-fluoranil's radical anion is longer (1.348 Å) than the C–F bond in the neutral *p*-fluoranil molecule (1.320 Å). For *p*-benzoquinone, bond distance changes are similar. The calculated CO distance is 0.041 Å longer for *p*-benzosemiquinone radical anion than for *p*-benzoquinone (1.263 Å vs 1.222 Å), the C2C2' distance is 0.028 Å longer for the radical anion than for the neutral molecule (1.369 Å vs 1.341 Å), and the CC2 distance is 0.032 Å shorter for *p*-benzosemiquinone radical anion than for *p*-benzoquinone (1.449 Å vs 1.481 Å). Consequently, for all three molecules—*p*-chloranil, *p*-fluoranil, and *p*-benzoquinone—bond distance changes upon reduction to their radical anions may be understood qualitatively from the nodal structure of *p*-benzoquinone's LUMO, obtained from a UHF calculation and sketched qualitatively in **4**. Occupying the MO in **4** with one electron should lengthen bonds characterized by an out-of-phase, antibonding interaction between neighboring atoms and shorten bonds characterized by an in-phase, bonding interaction. Thus, **4**

implies that reducing any *p*-benzoquinone with a LUMO similar to **4** by one electron should lengthen the CO and C2C2' bonds, while shortening the CC2 bond distances.



4

Although differences in calculated bond distance changes among the three molecules are small, the trend in calculated CO and C2C2' bond distance changes upon reducing the three quinones to their radical anions (*p*-chloranil < *p*-fluoranil < *p*-benzoquinone) may be rationalized by considering the MO sketched in **4**. Since π -bonding substituents should delocalize the single electron occupying the MO shown in **4** onto the substituents, strong π -bonding substituents should reduce the electron density on the carbon–oxygen framework in this MO and thus reduce the effect on bond distances of occupying the MO with one electron. Because π -bonding ability generally increases as electronegativity decreases, the electron occupying the MO in **4** should be concentrated on the carbon and oxygen atoms of *p*-benzosemiquinone radical anion, slightly delocalized away from the carbon–oxygen framework of *p*-fluoranil's radical anion and still more delocalized away from the carbon–oxygen framework of *p*-chloranil's radical anion. This delocalization should decrease CO and C2C2' π -antibonding interactions for the MO shown in **4** in the order *p*-chloranil < *p*-fluoranil < *p*-benzoquinone, the same order as the calculated trend in bond distance changes. Calculated changes in CC2 bond distances, however, illustrate the dangers in qualitatively explaining small differences in bond distances: the same argument would also predict calculated changes in CC2 distances in the same order, a trend that is not observed. If the above rationale for CO and C2C2' bond distance changes is correct, however, it would predict even smaller changes in CO and C2C2' bond distances for *p*-bromanil and *p*-iodanil than for *p*-chloranil. We have not studied either *p*-bromanil or *p*-iodanil by using these same methods, nor are sufficiently accurate experimental structures available for these molecules and their radical anions to test the proposed trend further.

Radical Anions of *p*-Chloranil, *p*-Fluoranil, and *p*-Benzoquinone: Spin Properties

To our knowledge, extensive experiments to characterize the spin density distribution in the radical anions of *p*-chloranil, *p*-fluoranil, and *p*-benzoquinone are available only for the *p*-benzosemiquinone radical anion⁴⁵ (see **3**). Unfortunately, both quantitative and qualitative agreement between atomic spin densities for *p*-benzosemiquinone radical anion derived from experiment and from Mulliken population analysis⁸⁴ and the largest basis set, denoted [632|41]^{72,73} in Table 4, is only fair: the oxygen atom is calculated to carry the largest spin density (0.259), but C2 and C are calculated to have equal spin densities of 0.084. Compared with the experimentally derived spin densities, the B3P86 calculations thus exaggerate the spin density on oxygen, underestimate the spin density on C, and slightly underestimate the spin density on C2. Other local DF, gradient-corrected DF, and hybrid HF/DF methods tested with the 6-31G(d) and [632|41] basis sets (including the B3LYP method) are similar to those calculated from the B3P86 method.

To investigate whether or not agreement between calculated and experimental spin densities could be improved for *p*-benzosemiquinone radical anion, we used a different method of calculating spin densities—Bader population analysis⁸⁶—and in addition tested the BLYP method with basis sets including

TABLE 4: Isotropic Hyperfine Coupling Constants and Spin Densities for the Radical Anions of *p*-Benzoquinones (C₆X₄O₂): *p*-Benzoquinone (X = H), *p*-Fluoranil (X = F), and *p*-Chloranil (X = Cl) Using the B3P86 Hybrid Hartree–Fock/Density Functional Method and Three Different Basis Sets. Hyperfine Coupling Constants Calculated at the B3LYP/[632|41]/B3LYP/6-31G(d) Level Are Also Reported for Radical Anions with X = H and X = F (the [632|41] Basis Set Is Currently Available for Chlorine)

atom	hyperfine coupling constants					B3P86-derived spin densities		
	B3P86/6-31G(d)	B3P86/6-311G(d,p)	B3P86/[632 41]	B3LYP/[632 41]// B3LYP/6-31G(d)	expt ^a	6-31G(d)	6-311G(d,p)	[632 41]
C	−0.30	−4.60	−4.11	−2.18	−2.13	0.062	0.064	0.084
O	−7.49	−3.98	−5.92	−7.77	−9.46	0.279	0.276	0.259
C2	1.80	−1.28	−0.56	−0.08	−0.12	0.085	0.086	0.084
X = H	−2.79	−2.23	−2.19	−2.18	−2.42	−0.006	−0.007	−0.005
C	−0.47	−4.38	−4.04	−3.70		0.079	0.080	0.085
O	−7.62	−3.74	−5.57	−7.46		0.285	0.281	0.268
C2	0.69	−1.63	−0.97	−0.49		0.062	0.064	0.067
X = F	2.78	1.95	2.13	2.54		0.006	0.005	0.007
C	−1.27	−4.63				0.052	0.054	
O	−7.40	−3.38				0.271	0.265	
C2	0.99	−0.21				0.083	0.085	
X = Cl	0.01	−0.08				0.005	0.005	

^a Sullivan, P. D.; Bolton, J. R.; Geiger, W. E. *J. Am. Chem. Soc.* **1970**, *92*, 4176–4180.

diffuse functions and more polarization functions. Although spin densities calculated by using the B3P86 method with Bader population analysis are very similar to those obtained by using Mulliken population analysis (atomic spins from Bader population analysis, the B3P86 method, and 6-31G(d) basis are $\rho(\text{O}) = 0.257$; $\rho(\text{C}) = 0.082$; $\rho(\text{C}2) = 0.081$), Bader's method correctly predicts that spin density on C is larger than the spin density on C2. Similarly, spin densities calculated by using the BLYP method with basis sets as large as 6-311++G(d,p) vary by less than 0.02 from those calculated by using the 6-31G(d) basis, but yield the correct relative magnitudes of the spin density on the atoms of *p*-benzosemiquinone radical anion. Of all the computational methods and basis sets tested, the ROHF method with the 6-31G(d) basis set actually predicts atomic spin densities in closest agreement with experiment. According to the ROHF method, the spin density on oxygen is 0.150, on C is 0.139, and on C2 is 0.105. Although we have not performed such extensive tests to reproduce accurate spin densities for the radical anion of *p*-chloranil, we find that the ROHF method gives the most accurate spin density on the only atom for which spin density has been reported—the radical's oxygen atom (observed $\rho(\text{O}) = 0.150$; ROHF/6-31G(d) $\rho(\text{O}) = 0.153$)—and the DF and HF/DF methods with the 6-31G(d) basis set all exaggerate the spin density on oxygen (for example, BLYP $\rho(\text{O}) = 0.251$). Since the ROHF method includes neither spin polarization nor correlation effects, the agreement between ROHF and experimentally derived spin densities is almost certainly fortuitous.

Table 4 also displays isotropic hyperfine coupling constants (hfcc's) for the radical anions of *p*-benzoquinone, *p*-fluoranil, and *p*-chloranil. Isotropic hyperfine coupling constants depend upon spin density at the position of a particular nucleus (the Fermi contact spin density, $\rho(\text{N})$) according to

$$a_o = \frac{8\pi}{3} g g_N \beta \beta_N \rho(\text{N})$$

where g is the electronic g factor, β is the electronic Bohr magneton, and g_N and β_N are the analogous values for nucleus N. Thus hfcc's provide an alternative, more direct and more stringent test of a method's ability to reproduce spin densities, independent of methods for population analysis. The isotropic proton hfcc for *p*-benzosemiquinone radical anion calculated by using both the UHF (−3.840) and UMP2 (−3.968) methods is larger than experiment (−2.419⁴⁵ or −2.425⁴⁵), the hfcc derived from B3P86 (−2.789) is slightly better, and that from

BP86 (−2.520) and B3LYP (−2.500) calculations is slightly too large. The hfcc from the SVWN method (−2.059) is too small. The gradient-corrected BLYP method gives the proton hfcc in best agreement with experiment (−2.460). Including diffuse functions in the basis set (6-31+G(d)) improves the proton hfcc to −2.400, but expanding the basis set further by adding more diffuse (6-31++G(d)) and polarization functions (6-31++G(d,p)) and finally changing to a triple- ζ valence basis (6-311+G(d), 6-311++G(d), and 6-311++G(d,p)) yields even poorer agreement with experiment than the 6-31+G(d) basis shows. The results obtained with expanded basis sets imply that expanding a basis set to improve the description of electron density in the valence region diffuses electron density away from the proton nucleus, to the detriment of attempts to estimate proton hfcc's. Results obtained with different DF and HF/DF methods are consistent with published results reporting that gradient-corrected DF and HF/DF methods give hfcc's in better agreement with experiment than local DF methods.^{88,89} In addition, heavy atom hfcc's determined by the B3P86/[632|41] method appear to agree well with the available experimental data, but are not as accurate as those derived from the B3LYP/[632|41]/B3LYP/6-31G(d) method.^{46–49} In summary, we must conclude that atomic spin densities calculated by using the BLYP method and basis sets at least as large as 6-31G+(d) agree qualitatively with experimentally derived spin densities; the proton hfcc derived from Fermi contact spin densities for *p*-benzosemiquinone radical anion are given accurately by a variety of methods and basis sets. Heavy atom hfcc's are reproduced qualitatively correctly by the B3P86/[632|41] method and basis set, whereas the B3LYP/[632|41] method and basis set give the best overall hfcc's of all methods tested here (using the B3LYP/6-31G(d) geometries).^{46–49}

Vibrations of *p*-Chloranil, *p*-Fluoranil, and *p*-Benzoquinone Radical Anions

Selected, calculated vibrational modes for *p*-chloranil and its radical anion—including the in-phase (a_g symmetry) and out-of-phase (b_{1u}) CO stretching modes, the in-phase (a_g) and out-of-phase (b_{2u}) C2C2' stretching vibrations, the b_{1u} symmetry CC2' stretching mode, and the a_g symmetry ring bending mode—are sketched in Figure 1, and their experimentally measured^{57,90} and calculated⁶² frequencies are listed to the upper right of each sketch. Calculated and experimental frequencies for the neutral *p*-chloranil molecule are listed at the upper left

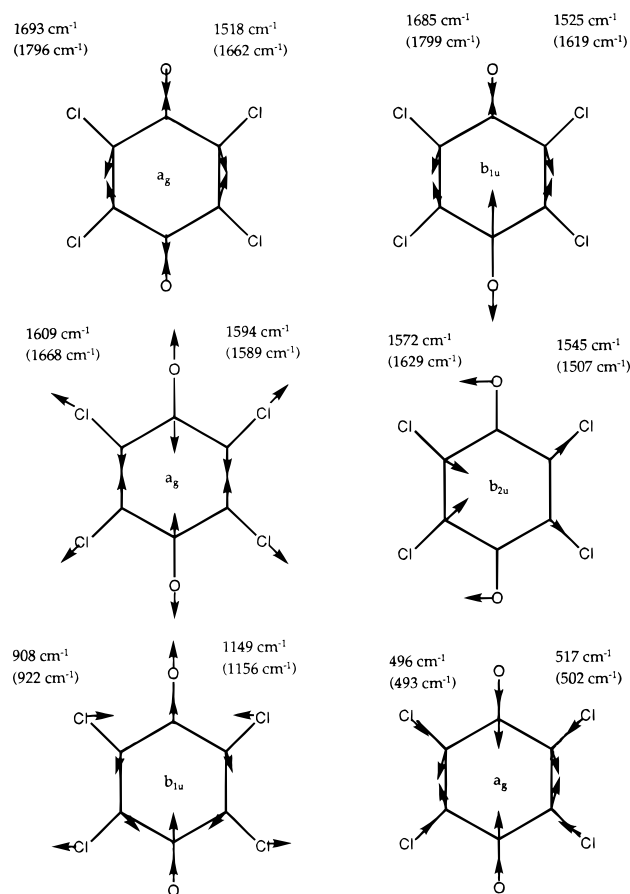


Figure 1. Selected vibrational modes of *p*-chloranil's radical anion. Frequencies for neutral *p*-chloranil are to the left of each drawing, frequencies for the radical anion are to the right. Experimentally measured frequencies (from ref 57) are given above calculated frequencies (in parentheses).

of each sketch. All calculated frequencies presented in the figure were obtained by using the B3P86 HF/DF method.

The highest frequency experimentally observed mode for *p*-chloranil is the in-phase a_g symmetry CO stretching mode observed at 1693 cm⁻¹ and calculated to appear at 1796 cm⁻¹. The out-of-phase b_{1u} symmetry CO stretch appears at 1685 cm⁻¹, immediately below the in-phase CO stretch. The calculated frequency for the out-of phase CO stretch, 1799 cm⁻¹, places it at a slightly higher frequency than the calculated in-phase CO stretch, in conflict with experiment. We have previously noted the difficulty experienced by DF and HF/DF methods in reproducing the relative frequencies for CO stretching modes of *p*-benzoquinones and believe it may be due to incorrect mixing between the a_g symmetry CO and C2C2' stretching modes. If the calculated mixing is too strong, the higher frequency CO stretch would appear too high. The next highest frequency mode of *p*-chloranil is the C2C2' stretching mode of a_g symmetry, experimentally measured at 1609 cm⁻¹ and calculated at 1668 cm⁻¹, followed by the b_{2u} symmetry C2C2' stretch observed at 1572 cm⁻¹ and calculated at 1629 cm⁻¹. The b_{1u} CC2 stretch appears significantly below the CO and C2C2' stretching modes, at an observed frequency of 908 cm⁻¹ and a calculated frequency of 922 cm⁻¹. Finally, the figure also shows the a_g symmetry, ring bending mode of *p*-chloranil radical anion, observed at 496 cm⁻¹ for the neutral *p*-chloranil molecule and calculated to appear at 493 cm⁻¹.

Comparing observed and calculated vibrational frequencies listed in Figure 1 for *p*-chloranil with those of its radical anion reflect changes in bonding expected upon reducing *p*-chloranil by one electron (see 1 and 2). Thus, the CO bond weakens

and both the a_g symmetry CO stretch (observed at 1518 cm⁻¹ and calculated at 1662 cm⁻¹) and the b_{1u} symmetry CO stretch (measured at 1525 cm⁻¹ and calculated at 1619 cm⁻¹) move to substantially lower frequencies compared to the corresponding modes of *p*-chloranil. Thus, the a_g symmetry CO stretching mode moves to a lower frequency than the b_{1u} symmetry CO stretch in *p*-chloranil's radical anion, but our calculations once again reverse the order of the CO stretching modes. Our B3P86 calculations also predict that both C2C2' stretching modes decrease in frequency, but place both C2C2' stretching modes below the CO stretches (the a_g symmetry mode is observed at 1594 cm⁻¹ and calculated at 1589 cm⁻¹; the b_{2u} symmetry mode is observed at 1545 cm⁻¹ and calculated at 1507 cm⁻¹). So even if strong mixing between the two a_g symmetry modes results in reversing the two mode assignments, the b_{2u} symmetry C2C2' mode still appears at too low a frequency. Of the computational methods tested (B3P86, B3LYP, BLYP, SVWN, and UHF), none correctly reproduces the relative order of these four modes: the two CO stretches and the two C2C2' stretches.

Calculated frequencies for the CC2 stretch and the a_g ring bending mode of *p*-chloranil's anion agree well with experimental measurements, and both modes shift to higher frequencies relative to the corresponding modes of the neutral *p*-chloranil molecule. First, the CC2 stretching mode is observed at 1149 cm⁻¹ and calculated to appear at 1156 cm⁻¹ and to contain a substantial contribution from C-Cl stretching motions. The experimentally observed mode thus shifts up in frequency by 241 cm⁻¹ and the calculated frequency increases by 234 cm⁻¹ upon reducing *p*-chloranil to its radical anion. Similarly, the ring stretching mode observed at 517 cm⁻¹ for the anion is calculated at 502 cm⁻¹. Compared with *p*-chloranil, the experimental frequency increases by 21 cm⁻¹ and the calculated frequency increases by 9 cm⁻¹.

Below the CO and C2C2' stretches, but above the CC2 and ring stretches, we calculate three additional C-Cl stretching modes that have been experimentally measured for *p*-chloranil's radical anion. First, the a_g symmetry C-Cl stretch calculated at 1028 cm⁻¹ matches most closely the C-Cl stretch observed at the same frequency and is actually a mixture of CC2 and C-Cl stretching vibrations. The next highest C-Cl stretch, of b_{2u} symmetry, is calculated at 719 cm⁻¹ and observed at 722 cm⁻¹. Finally, the lowest frequency C-Cl stretching mode (b_{1u} symmetry) is calculated at 455 cm⁻¹ and observed at 468 cm⁻¹. Thus, all experimentally observed C-Cl stretching frequencies are well reproduced by our calculations.

Other calculated frequencies corresponding to experimentally observed modes include a mixed CC and C-Cl stretching mode calculated at 917 cm⁻¹ (experimentally observed at 918 cm⁻¹), a C-Cl wag calculated at 711 cm⁻¹ (corresponding to an experimentally assigned CO bend observed at 695 cm⁻¹), and a CO bend calculated and observed at 374 cm⁻¹. A ring bend of a_g symmetry was calculated at a lower frequency of 334 cm⁻¹ (observed at 338 cm⁻¹). The three lowest frequency modes of *p*-chloranil's radical anion were calculated to be C-Cl bending modes. They have b_{3u} , b_{2u} , and b_{1u} symmetry, and their frequencies are 214 cm⁻¹ (experimental frequency of 212 cm⁻¹), 208 cm⁻¹ (experimental frequency of 200 cm⁻¹), and 187 cm⁻¹ (experimental frequency of 220 cm⁻¹), respectively. Thus, these low-frequency modes appear at calculated frequencies in excellent agreement with experimentally observed frequencies.

In summary, the average agreement between experiment and calculation is very good for *p*-chloranil's radical anion. The average absolute difference between experimental and B3P86-derived frequencies is only 24 cm⁻¹. The differences between observed and calculated frequencies range from 0 cm⁻¹ for a

TABLE 5: Symmetries, Approximate Mode Descriptions, and Unscaled Harmonic Vibrational Frequencies (cm⁻¹) for the Radical Anions of *p*-Benzoquinone, *p*-Fluoranil, and *p*-Chloranil Determined by the B3P86 Hybrid Hartree–Fock/Density Functional Method and Using a 6-31G(d) Basis Set

sym	approximate description	X = H	approximate descriptions	X = F	approximate descriptions	X = Cl
a _g	C–H str	3181	C–F str	1279	C–Cl str C–C str	1028
b _{2u}	C–H str	3175	C–F str	997	C–Cl str	719
b _{3g}	C–H str	3154	C–F str	1123	C–Cl str	846
b _{1u}	C–H str	3153	C–F str	1355	C–Cl str, C–C str	455
b _{1u}	C=O str	1597	C=O str	1607	C=O str	1619
a _g	C=O str	1548	C=O str	1627	C=O str	1662
a _g	C=C str	1709	C=C str	1716	C=C str	1589
b _{2u}	C=C str	1534	C=C str	1619	C=C str	1507
b _{3g}	C–C str	1473	C–F str, C–C str	1472	C–C str	1358
b _{1u}	C–H bend	1387	C–F bend	312	C–Cl bend	208
b _{2u}	C–C str	1248	C–C str	1266	C–C str	1162
b _{3g}	C–H bend	1264	C=O bend, C–F bend	279	C–Cl bend	332
a _g	C–H bend	1158	C–F bend	265	C–Cl bend	201
b _{2u}	C–H bend	1080	C–F bend	281	C–Cl bend	214
b _{2g}	C–H wag	946	C–F wag	154	C–Cl wag	113
a _u	C–H wag	941	C–F wag	125	C–Cl wag	70
b _{1u}	C–C=C bend	969	C–C str, C–F bend	1070	C–C str	917
b _{3u}	C–H wag	859	C–F wag	206	C–Cl wag	187
a _g	C–C str	832	ring breathing	565	ring breathing	334
b _{2g}	ring chair bend	800	ring chair bend	565	ring chair bend	736
b _{1u}	C–C str	795	C–C=C bend	610	C–Cl str, C–C str	1156
b _{1g}	C–H wag	773	C–F wag	352	C–Cl wag	324
b _{3g}	C=O bend, C–C str	633	C–C=C bend	426	C–C=C bend, C–O bend	277
b _{3u}	ring boat bend	519	ring boat bend	673	ring boat bend	711
a _g	C–C–C bend	469	C–C–C bend	436	C–C–C bend	502
b _{3g}	C=O bend	466	C–F bend, C=O bend	799	C=O bend, C–Cl bend	726
b _{2u}	C=O bend	391	C=O bend	342	C=O bend	362
a _u	C=C–C bend	393	C=C–C bend	551	C=C–C bend	546
b _{2g}	C=O chair bend	328	C=O chair bend	368	C=O chair bend	386
b _{3u}	C=O boat bend	139	C=O boat bend	109	C=O boat bend	78

C–Cl stretch to 144 cm⁻¹ for a CO stretching mode. All computational methods tested fail to reproduce the experimentally determined order of the CO and C2C2' stretching modes for *p*-chloranil's radical anion, so either the experimentally determined mode assignments or all quantum chemical methods tested here are incorrect on this point.

Table 5 also presents the calculated vibrational frequencies and their mode assignments for the radical anions of *p*-fluoranil and *p*-benzoquinone, for comparison with experiment and with those of *p*-chloranil's radical anion. Only two modes have been experimentally observed for *p*-fluoranil's anion, the in-phase, a_g symmetry C2C2' stretch observed at 1677 cm⁻¹ and calculated at 1716 cm⁻¹ and the a_g symmetry CO stretch observed at 1556 cm⁻¹ and calculated to appear at 1627 cm⁻¹. For *p*-fluoranil's radical anion, the numerical agreement between calculation and experiment appears comparable to that for the radical anion of *p*-chloranil, except that our calculations reproduce the correct relative order of the CO and C2C2' stretching frequencies for the *p*-fluoranil radical anion. We note that the b_{2u} symmetry C2C2' stretching mode is calculated to appear at 1619 cm⁻¹ and the b_{1u} symmetry CO stretch is calculated at 1607 cm⁻¹. For *p*-benzoquinone radical anion, the highest frequency CO stretch (b_{1u} symmetry) is calculated at 1597 cm⁻¹ and was not experimentally observed. Immediately below the b_{1u} CO stretching mode is the a_g stretch, at a calculated frequency of 1548 cm⁻¹, in moderately good agreement with the experimental frequency of 1435 cm⁻¹. The C2C2' stretching modes appear immediately below the CO stretching modes, at calculated frequencies of 1693 cm⁻¹ (experimentally observed at 1620 cm⁻¹) and 1534 cm⁻¹. Other experimentally observed modes and their frequencies include a CH bending mode calculated at 1158 cm⁻¹ (observed at 1161 cm⁻¹) and the ring CCC bend calculated at 469 cm⁻¹ (observed at 481 cm⁻¹). Thus, for the radical anions of *p*-fluoranil and *p*-benzoquinone, calculated frequencies differ from experimen-

tally measured frequencies by magnitudes similar to those for *p*-chloranil's anion. For *p*-fluoranil's and *p*-benzoquinone's radical anions, however, the B3P86 method also reproduces the correct relative order of the CO and C2C2' stretching frequencies. We also note that both the b_{1u} and a_g symmetry CO stretching modes increase in frequency with increasing strength of the substituent π bonding, in the order *p*-benzosemiquinone anion < *p*-fluoranil anion < *p*-chloranil anion. Since the singly occupied MO of each anion is CO antibonding, the trend of increasing calculated CO stretching frequencies reflects the increasing delocalization of the unpaired electron onto the substituents and away from the CO bond.

Conclusions

Structures, spin properties, and vibrations for the anions of *p*-benzoquinone, *p*-fluoranil, and *p*-chloranil were calculated by using a variety of density-functional-based methods. The structure of neutral *p*-chloranil, calculated by using the B3P86 hybrid Hartree–Fock/density functional and 6-31G(d) basis set, agrees within experimental error with the published electron diffraction structure, and bond distance changes upon reducing the molecule to its radical anion are consistent with resonance structures indicating a shift toward a more phenolic structure. Structural changes upon reducing *p*-benzoquinone and *p*-fluoranil to their semiquinone anions are similar and are understandable based on *p*-benzoquinone's LUMO. Trends in calculated C=O and C=C bond distance changes upon reducing the three molecules to their radical anions (*p*-chloranil < *p*-fluoranil < *p*-benzoquinone) follow a pattern expected from π -bonding abilities of the substituents, set by their relative electronegativities.

Spin properties for the three radical anions were also calculated by using a variety of methods and basis sets, including Chipman's [632|41] basis set^{72,73} designed to give accurate hyperfine properties in MO calculations. Spin densities for the

p-benzosemiquinone radical anion calculated by using the B3P86/[632|41]/B3P86/6-31G(d) method show only qualitative agreement with experiment, whereas isotropic proton hyperfine coupling constants (hfcc's) were calculated accurately by using a variety of gradient-corrected and hybrid HF/DF methods. In addition, heavy atom hfcc's were reproduced qualitatively by the B3P86/[632|41] method, but slightly better accuracy was achieved by using the B3LYP/[632|41]/B3LYP/6-31G(d) method. Finally, comparing hfcc's calculated with a variety of different basis sets illustrates that expanding the basis set in the valence region diffuses electron density away from the nucleus and, in many cases, results in poorer agreement with experiment.

Calculated vibrational frequencies and mode assignments for the radical anions of *p*-benzoquinone, *p*-fluoranil, and *p*-chloranil are also presented, and the modes of *p*-chloranil are compared with those of its radical anion. For neutral *p*-chloranil, calculated frequencies agree well with experiment, except that the relative order of the a_g and b_{1u} C=O stretching modes is reversed. Calculated vibrational frequency shifts upon reducing *p*-chloranil to its radical anion are consistent with shifts expected from the molecule's LUMO, but once again the relative order of the CO stretching modes is reversed compared to experiment, and calculations also place the C2C2' stretches at higher frequencies than the CO stretches, in conflict with experiment. In contrast, calculated CO and C2C2' vibrational frequencies for the anions of *p*-benzoquinone and *p*-fluoranil appear in the correct relative order and their vibrational frequencies display an average absolute difference from experiment comparable to that calculated for *p*-chloranil's radical anion (24 cm⁻¹). We also note that both the b_{1u} and a_g symmetry CO stretching modes increase in frequency with increasing strength of substituent π bonding, in the order *p*-benzosemiquinone anion < *p*-fluoranil anion < *p*-chloranil anion. Since the singly occupied MO of each anion is CO antibonding, the trend of increasing calculated CO stretching frequencies reflects the increasing delocalization of the unpaired electron onto the substituents and away from the CO bond. Thus, our calculations reproduce qualitative features of vibrational frequencies and display small absolute average differences from experiment, but fail to reproduce the correct relative ordering of C=C vs CO stretching modes for *p*-chloranil's radical anion, as well as the order of the two CO stretches for both *p*-chloranil and its radical anion.

Acknowledgment. The research discussed in this publication was made possible by OCAST award number H97-091, from the Oklahoma Center for the Advancement of Science and Technology, NSF award number OST-9550478 to the Center for Photonic and Electronic Materials and Devices, and supercomputer time grants from the NSF/MetaCenter Allocations Committee (award number MCA96N019), the NSF/National Center for Supercomputing Applications, and the NSF/Cornell Theory Center. The Cornell Theory Center receives major funding from the NSF and New York State. Additional funding comes from the ARPA, the NIH, IBM Corp., and other members of the center's Corporate Research Institute. We are also grateful for supercomputer time at the University of Oklahoma made possible by support from IBM Corporation (in part through a Share University Research grant), Silicon Graphics Inc., and the University of Oklahoma.

Supporting Information Available: Tables of geometries and vibrational frequencies of *p*-benzoquinone, *p*-fluoranil, and *p*-chloranil calculated by using the 6-31G(d) basis set and a variety of quantum chemical methods: unrestricted Hartree-Fock (UHF), second-order Møller-Plesset perturbation theory (MP2), the SVWN local density functional, BLYP gradient-

corrected density functional and B3LYP hybrid Hartree-Fock/density functional methods (5 pages). Ordering information is given on any current masthead page.

References and Notes

- Connolly, J. S.; Bolton, J. R. In *Photoinduced Electron Transfer*; Fox, M. A., Chanon, M., Eds.; Elsevier: Amsterdam, 1988; Vol. D, pp 303ff.
- Ebersson, L. *Electron-Transfer Reactions in Organic Chemistry*; Springer-Verlag: Berlin, 1987.
- Bernstein, J.; Cohen, M. D.; Leiserowitz, L. In *The Chemistry of Quinonoid Compounds*; Patai, S., Ed.; John Wiley & Sons: Chichester, 1974; pp 37-110.
- Foster, R. *Organic Charge-Transfer Complexes*; Academic: London, 1969.
- Foster, R.; Foreman, M. I. In *The Chemistry of Quinonoid Compounds*; Patai, S., Ed.; John Wiley & Sons: Chichester, 1974; pp 257-333.
- Depew, M. C.; Wan, J. K. S. In *The Chemistry of Quinonoid Compounds*; Patai, S., Rappaport, Z., Eds.; John Wiley & Sons: Chichester, 1988; Vol. II, pp 963-1018.
- Function of Quinones in Energy Conserving Systems*; Trumpower, B. L., Ed.; Academic: New York, 1982.
- Dryhurst, G.; Kadish, K. M.; Schneller, F.; Renneberg, R. *Biological Electrochemistry*; Academic Press: New York, 1982.
- Stryer, L. *Biochemistry*, 3rd ed.; W. H. Freeman & Co.: New York, 1988.
- Brandt, U.; Trumpower, B. *Crit. Rev. Biochem. Mol. Biol.* **1994**, *29*, 165-197.
- Trumpower, B. L.; Gennis, R. B. *Annu. Rev. Biochem.* **1994**, *63*, 675-716.
- Hubig, S. M.; Bockman, T. M.; Kochi, J. K. *J. Am. Chem. Soc.* **1997**, *119*, 2926-2935.
- Breton, J.; Nabedryk, E. *Biochim. Biophys. Acta* **1996**, *1275*, 84-90, and references therein.
- Mäntele, W. In *Anoxygenic Photosynthetic Bacteria*; Blankenship, R. E., Madigan, M. T., Bauer, C. E., Eds.; Kluwer: Dordrecht, 1995; pp 627-647.
- Angerhofer, A.; Bittl, R. *Photochem. Photobiol.* **1996**, *63*, 11-38, and references therein.
- MacMillan, F.; Lenzian, F.; Lubitz, W. *Magn. Reson. Chem.* **1995**, *33*, S81-S93.
- Hagen, K.; Hedberg, K. *J. Chem. Phys.* **1973**, *59*, 158-162.
- Hagen, K.; Hedberg, K. *J. Mol. Struct.* **1978**, *49*, 351-360.
- Hagen, K.; Nicholson, D. G. *Acta Crystallogr.* **1987**, *C43*, 1959-1961.
- Kimura, M.; Shibata, S. *Bull. Chem. Soc. Jpn.* **1954**, *27*, 163-166.
- Schei, H.; Hagen, K.; Traetteberg, M. *J. Mol. Struct.* **1980**, *62*, 121-130.
- Swingle, S. M. *J. Am. Chem. Soc.* **1954**, *76*, 1409-1411.
- Trotter, J. *Acta Crystallogr.* **1960**, *13*, 86-95.
- Ueda, I. *J. Phys. Soc. Jpn.* **1961**, *16*, 1185-1194.
- van Weperen, K. J. *Acta Crystallogr.* **1972**, *B28*, 338-342.
- Meresse, A.; Courseille, C.; Chanh, N. B. *Acta Crystallogr.* **1974**, *B3*, 524-526.
- Chu, S. S. C.; Jeffrey, G. A.; Sakurai, T. *Acta Crystallogr.* **1962**, *15*, 661-671.
- Boer, J. L. d.; Vos, A. *Acta Crystallogr.* **1963**, *B24*, 720-730.
- Anno, T. *J. Chem. Phys.* **1965**, *42*, 932-941.
- Becker, E. D.; Charney, E.; Anno, T. *J. Chem. Phys.* **1965**, *42*, 942-949.
- Becker, E. D. *J. Phys. Chem.* **1991**, *95*, 2818-2823.
- Charney, E.; Becker, E. D. *J. Chem. Phys.* **1965**, *42*, 910-913.
- Deschamps, J.; Lafore, M.-L.; Etchepare, J.; Chaillet, M. *J. Chim. Phys. Phys.-Chim. Biol.* **1970**, *67*, 722-730.
- Girlando, A.; Pecile, C. *J. Chem. Soc., Faraday Trans. 2* **1973**, *69*, 1291-1303.
- Girlando, A.; Pecile, C. *J. Chem. Soc., Faraday Trans. 2* **1975**, *71*, 689-698.
- Girlando, A.; Pecile, C. *J. Mol. Spectrosc.* **1979**, *77*, 374-384.
- Kubinyi, M.; Keresztury, G. *Spectrosc. Acta A* **1989**, *45A*, 421-429.
- Palmo, K.; Pietila, L.-O.; Mannfors, A.; Karonen, A.; Stenman, F. *J. Mol. Spectrosc.* **1983**, *100*, 368-376.
- Pietila, L.-O.; Palmo, K.; Mannfors, B. *J. Mol. Spectrosc.* **1986**, *116*, 1-16.
- Trommsdorff, H. P.; Wiersma, D. A.; Zelsmann, H. R. *J. Chem. Phys.* **1985**, *82*, 48-52.
- Yamada, H.; Saheki, M.; Fukushima, S.; Nagasao, T. *Spectrochim. Acta* **1974**, *30A*, 295-309.
- Dunn, T. M.; Francis, A. H. *J. Mol. Spectrosc.* **1974**, *50*, 1-13.
- Stammreich, H.; Sans, T. T. *J. Chem. Phys.* **1965**, *42*, 920-931.

- (44) Konno, M.; Kobayashi, H.; Marumo, F.; Saito, Y. *Bull. Chem. Soc. Jpn.* **1973**, *46*, 1987–1990.
- (45) Prabhananda, B. S. *J. Chem. Phys.* **1983**, *79*, 5752–5757.
- (46) Boesch, S. E.; Wheeler, R. A. *J. Phys. Chem. A* **1997**, *101*, 5799–5804.
- (47) Wise, K. E.; Grafton, A. K.; Wheeler, R. A. *J. Phys. Chem. A* **1997**, *101*, 1160–1165.
- (48) Grafton, A. K.; Boesch, S. E.; Wheeler, R. A. *J. Mol. Struct. (THEOCHEM)* **1997**, *392*, 1–11.
- (49) Grafton, A. K.; Wheeler, R. A. *J. Phys. Chem. A* **1997**, *101*, 7154–7166.
- (50) Qin, Y.; Wheeler, R. A. *J. Am. Chem. Soc.* **1995**, *117*, 6083–6092.
- (51) Qin, Y.; Wheeler, R. A. *J. Chem. Phys.* **1995**, *102*, 1689–1698.
- (52) Walden, S. E.; Wheeler, R. A. *J. Chem. Soc., Perkin Trans. 2* **1996**, 2663–2672.
- (53) Walden, S. E.; Wheeler, R. A. *J. Am. Chem. Soc.* **1997**, *119*, 3175–3176.
- (54) Tripathi, G. N. R. *J. Chem. Phys.* **1981**, *74*, 6044–6049.
- (55) Tripathi, G. N. R.; Schuler, R. H. *J. Phys. Chem.* **1983**, *87*, 3101–3105.
- (56) Schuler, R. H.; Tripathi, G. N. R.; Prebenda, M. F.; Chipman, D. M. *J. Phys. Chem.* **1983**, *87*, 5357–5361.
- (57) Girlando, A.; Zanon, I.; Bozio, R.; Pecile, C. *J. Chem. Phys.* **1978**, *68*, 22–31.
- (58) Labanowski, J. K.; Andzelm, J. W. *Density Functional Methods in Chemistry*; Springer-Verlag: New York, 1991.
- (59) Parr, R. G.; Wang, W. *Density-Functional Theory of Atoms and Molecules*; Oxford University Press: New York, 1989.
- (60) Becke, A. D. *J. Chem. Phys.* **1993**, *98*, 1372–1377.
- (61) Boesch, S. E. Thesis, The University of Oklahoma, 1996.
- (62) Boesch, S. E.; Wheeler, R. A. *J. Phys. Chem.* **1995**, *99*, 8125–8134.
- (63) Boesch, S. E.; Grafton, A. K.; Wheeler, R. A. *J. Phys. Chem.* **1996**, *100*, 10083–10087.
- (64) Qin, Y.; Wheeler, R. A. *J. Phys. Chem.* **1996**, *100*, 10554–10563.
- (65) Walden, S. E.; Wheeler, R. A. *J. Phys. Chem.* **1996**, *100*, 1530–1535.
- (66) Slater, J. C. *Quantum Theory of Molecules and Solids*; McGraw-Hill: New York, 1974; Vol. 4.
- (67) Becke, A. D. *Phys. Rev. A* **1988**, *38*, 3098–3100.
- (68) Vosko, S. H.; Wilk, L.; Nusair, M. *Can. J. Phys.* **1980**, *58*, 1200–1211.
- (69) Lee, C.; Yang, W.; Parr, R. G. *Phys. Rev. B* **1988**, *37*, 785–789.
- (70) Hehre, W. J.; Radom, L.; Schleyer, P. v. R.; Pople, J. A. *Ab initio Molecular Orbital Theory*; John Wiley & Sons: New York, 1986.
- (71) Helgaker, T.; Taylor, P. R. In *Modern Electronic Structure Theory, Part II*; Yarkony, D. R., Ed.; World Scientific: Singapore, 1995; Vol. 2, pp 725–856.
- (72) Chipman, D. M. *Theor. Chim. Acta* **1989**, *76*, 73–84.
- (73) Basis set was obtained from the Extensible Computational Chemistry Environment Basis Set Database, V., as developed and distributed by the Molecular Science Computing Facility, Environmental and Molecular Sciences Laboratory, which is part of the Pacific Northwest Laboratory, P.O. Box 999, Richland, WA 99352, and funded by the U.S. Department of Energy. The Pacific Northwest Laboratory is a multiprogram laboratory operated by Battelle Memorial Institute for the U.S. Department of Energy under contract DE-AC06-76RLO 1830. Contact David Feller, Karen Schuchardt, or Don Jones for further information.
- (74) Levine, I. N. *Quantum Chemistry*; 4th ed.; Prentice Hall: Englewood Cliffs, NJ, 1993.
- (75) Szabo, A.; Ostlund, N. S. *Modern Quantum Chemistry: Introduction to Advanced Electronic Structure Theory*; 1st ed.; revised ed.; McGraw-Hill Publishing Co.: New York, 1989.
- (76) Hohenberg, P.; Kohn, W. *Phys. Rev. B* **1964**, *136*, 864–871.
- (77) Kohn, W.; Sham, L. J. *Phys. Rev. A* **1965**, *140*, 1133–1138.
- (78) Frisch, M. J.; Trucks, G. W.; Head-Gordon, M.; Gill, P. M. W.; Wong, M. W.; Foresman, J. B.; Johnson, B. G.; Schlegel, H. B.; Robb, M. A.; Replogle, S.; Gomperts, R.; Andres, J. L.; Raghavachari, K.; Binkley, J. S.; Gonzalez, C.; Martin, R. L.; Fox, D. J.; Defrees, D. J.; Baker, J.; Stewart, J. J. P.; Pople, J. A. *GAUSSIAN92/DFT*; Gaussian, Inc.: Pittsburgh, 1992.
- (79) Frisch, M. J.; Trucks, G. W.; Schlegel, H. B.; Gill, P. M. W.; Johnson, B. G.; Robb, M. A.; Cheeseman, J. R.; Keith, T. A.; Petersson, G. A.; Montgomery, J. A.; Raghavachari, K.; Al-Laham, M. A.; Zakrzewski, V. G.; Ortiz, J. V.; Foresman, J. B.; Cioslowski, J.; Stefanov, B. B.; Nanayakkara, A.; Challacombe, M.; Peng, C. Y.; Ayala, P. Y.; Chen, W.; Wong, M. W.; Andres, J. L.; Replogle, E. S.; Gomperts, R.; Martin, R. L.; Fox, D. J.; Binkley, J. S.; Defrees, D. J.; Baker, J.; Stewart, J. J. P.; Head-Gordon, M.; Gonzalez, C.; Pople, J. A. *GAUSSIAN94* (Revision B.3); Gaussian, Inc.: Pittsburgh, 1995.
- (80) Lebedev, V. I. *Zh. Vychisl. Mater. Mater. Fiz.* **1975**, *15*, 48–54.
- (81) Lebedev, V. I. *Zh. Vychisl. Mater. Mater. Fiz.* **1976**, *16*, 293–306.
- (82) Schlegel, H. B. *J. Comput. Chem.* **1986**, *3*, 214–218.
- (83) Scott, A. P.; Radom, L. *J. Phys. Chem.* **1996**, *100*, 16502–16513.
- (84) Mulliken, R. S. *J. Chem. Phys.* **1955**, *23*, 1833–1840.
- (85) Mulliken, R. S.; Ermler, W. C. *Diatom Molecules*; Academic: New York, 1977.
- (86) Bader, R. F. W. *Atoms in Molecules: A Quantum Theory*; Oxford University Press: Oxford, 1990.
- (87) Cabana, A.; Bachand, J.; Giguere, J. *Can. J. Phys.* **1974**, *52*, 1949–1955.
- (88) Malkin, V. G.; Malkina, O. L.; Eriksson, L. A.; Salahub, D. R. In *Modern Density Functional Theory: A Tool for Chemistry*; Seminario, J. M., Politzer, P., Eds.; Elsevier: Dordrecht, 1995; Vol. 2, pp 273–347.
- (89) Barone, V. In *Recent Advances in Computational Chemistry, Vol. 1, Part I*; Chong, D. P., Ed.; World Scientific: Singapore, 1996.
- (90) Girlando, A.; Bozio, R.; Pecile, C. *J. Chem. Soc., Chem. Commun.* **1974**, 87–88.